## Original Article
# A novel, small peptide with activity against human pancreatic cancer

Michael R Kozlowski[1], Roni E Kozlowski[2]

[1]Arizona College of Optometry, Midwestern University, Glendale, Arizona, United States of America; [2]Kalos Therapeutics Incorporated, Phoenix, Arizona, United States of America

**Abstract:** KTH-222 is a novel, 8-amino acid length peptide. It is derived from a motif identified in a group of peptides that are related to atrial natriuretic peptide and that are able to inhibit cancer cell growth. We report here that KTH-222 inhibits the attachment, proliferation, and development of an invasive morphology in cultured human pancreatic tumor cells (MIA PaCa-2 and HPAC). At a biochemical level, it inhibits tubulin polymerization which may underlie these cellular effects. We further report that KTH-222 reduces the rate of tumor growth and prolongs survival in mice implanted with MIA PaCa-2 cells. In this model system, KTH-222 is more effective than gemcitabine, a drug commonly used in the treatment of pancreatic cancer. Furthermore, KTH-222 does not decrease the rate of weight gain in the treated mice, suggesting the absence of gross toxicity. These activities of KTH-222 suggest that it may be useful in the treatment of pancreatic cancer.

**Keywords:** Pancreatic cancer, chemotherapy, small peptide, atrial natriuretic peptide

## Introduction

Pancreatic cancer is the third leading cause of cancer-related deaths in the United States, with a 5-year survival rate of only 4% to 7% [1]. One of the recommended treatments for advanced pancreatic cancer is chemotherapy with gemcitabine, an antimetabolite, in combination with protein-bound paclitaxel, a tubulin inhibitor [2-4]. While initially very effective, the long-term utility of this regimen is ultimately limited by toxicity and the development of resistance. Thus, there is a need for newer drugs or drug combinations to treat this disorder [4-8].

Atrial natriuretic peptide (ANP), as well as certain natural and synthetic peptides related to it by sequence homology [9, 10] or by being derived from the same precursor protein [11], have been reported to inhibit pancreatic cancer cell growth *in vitro* [11-13]. Members of this group of peptides also inhibit the proliferation of cells derived from human lung, hepatic, and gastric cancers in culture [9-16]. Furthermore, ANP and these related peptides have been found to reduce the growth of tumors derived from human pancreatic cells as well as those from human breast and lung cancer cell in mouse xenograft models [11, 17-19]. ANP itself has also been reported to reduce metastases after curative lung cancer surgery in human clinical studies [20]. Taken together, these data point to potential utility for ANP and related peptides in the treatment of cancer.

Surprisingly, ANP and some of its related peptides including long-acting ANP (LANP), kaliuretic peptide (KP), and vessel dilator peptide (VDL), all of which inhibit the growth of cancer cells, share little sequence homology [11]. It has been possible, however, to identify a broadly defined motif that is common to all of these peptides [21]. This motif is 8 amino acids in length with moderately conserved residues at certain key positions. Screening of a library of peptides based on this motif with variations in the residues at each position produced a model of the optimal motif, from which KTH-222 was ultimately derived. In this report we describe the effectivness of KTH-222 in inhibiting the growth of human pancreatic cancer cells both in culture and in a mouse

**Table 1.** The common motif identified among ANP and related peptides that inhibit cancer cell growth is aligned with the sequences of ANP and the related peptides from which it was derived

| Peptide | Amino Acids Comprising Motif | Amino Acids at Each Residue in Motif | | | | | | | |
|---|---|---|---|---|---|---|---|---|---|
| | | 1 | 2 | 3 | 4 | 5 | 6 | 7 | 8 |
| CommonMotif | --- | HP, NP, NI | P, PC | P, NC | Any | HP, NP, NI | Non-HP | Any | HP, NP, NI |
| ANP | 8-15 | F | G | G | R | M | D | R | I |
| KP | 8-15 | L | K | S | K | L | R | A | L |
| LANP | 15-22 | F | K | N | L | L | D | H | L |
| VDL | 15-22 | A | G | A | A | L | S | P | L |
| Peptide Library | --- | A, F, L | G, K | A, G, L, N, S | *all* | L, M | D, R, S | *all* | I, L |
| KTH-222 | --- | L | K | G | Q | L | R | C | I |

Comparisons are also shown with the amino acids represented in the peptide library and the sequence of KTH-222. Characteristics used to describe allowable amino acid side chains in the conserved regions of the motif are: hydrophobic (HP), non-polar (NP), non-ionizable (NI), polar (P) and positively charged (PC).

tumor xenograft model. These data suggest that KTH-222 may be useful in the treatment of pancreatic cancer.

## Materials and methods

### Materials

KTH-222 ($NH_2$-LKGQLRCI-$CO_2$H) was synthesized at > 95% purity by New England Peptides (Gardner, MA). VDL ($NH_2$-EVVPPQLSEPNEE AGAALSPLPEVPPWTGEVSPAQR-$CO_2$H) was purchased from Phoenix Pharmaceuticals, Incorporated (Burlingame, CA) also at 95% purity. A library of 96 peptides ("peptide library") was designed based on an 8-amino acid motif common to ANP, VDL, KP, and LANP (**Table 1**). It was also synthesized at 95% purity by New England Peptides. All peptides were stored lyophilized at 4°C and dissolved just prior to use in either saline for the xenograft study or in phosphate-buffered saline (PBS) with 0.1% bovine serum albumin (BSA) for cellular studies. Peptides of the peptide library were reconstituted in 96 well plates and frozen after use. The frozen samples were thawed and re-used to confirm activity. Gemcitabine was received as a colorless solution and was stored at 4°C until use. Gemcitabine was diluted just prior to use in a saline solution. HPAC human pancreatic adenocarcinoma cells (CRL-2119) and MIA PaCa-2 human pancreatic epithelial cells (CRL-1420) were received from the American Type Culture Collection (ATCC; Manassas, VA), and were cultured according to the supplier's instructions. Following an initial expansion when first received, these cells were frozen back in aliquots for later use. For the current study,

a new aliquot was thawed, and the cells were carried for up to 4 passages (5 passages since they were received from ATCC). The cells were cultured in T25 flasks, and the medium was replaced twice weekly. The cells were split 1:10 into new flasks weekly. Before they reached confluence, the cells were dissociated with trypsin (15 minutes at 37°C), triturated (25 times using a 5 ml pipet), and used to seed either 6- or 24-well microtiter plates (see below).

### Cell culture

HPAC and MIA PaCa-2 cells were grown in microtiter plates (Corning™ Costar™ flat bottom cell culture microplate, Fisher Scientific, Waltham, MA). The cells were seeded either in 6-well plates at high density ($5 \times 10^5$ cells per well) or in 24-well plates at low density ($7 \times 10^3$ cells per well). KTH-222, or its vehicle (PBS with 0.1% BSA) was added to each well at the time of seeding. For some of the 6-well plates, the non-attached cells (i.e. those still in the medium) in each well were counted 3 hours after plating by withdrawing a small portion of the medium after gently rinsing the plate. For other 6-well plates, 24 h after the seeding of cells each well was washed and treated with trypsin, and the number of cells counted. All counting was done in triplicate using a Countess® automated cell counter (Thermo Fisher Scientific, Waltham, MA), and trypan blue dye exclusion was used to assess viability. For the 24-well plates, 24 hours after the seeding of cells, each well of the plates was washed with phosphate buffered saline, fixed with ethanol (0°C), and stained with crystal violet within the

wells for microscopic examination. For evaluation of cell morphology, three photomicrographs were made of each of the fixed and stained wells using Moticam-5 digital camera attached to a Motif 160 M inverted trinocular microscope (VWR, Radnor, PA). The field size was 1110 um by 830 um.

*Screening of the peptide library*

HPAC cells cultured in 24 well microtiter plates as described above were each exposed to a different peptide from the peptide library, or the vehicle (PBS with 0.1% BSA). The test substance was added to each well at the same time at a 1:1000 dilution, which gave a final concentration of 100 nM for the peptides. Twenty-four hours after adding the peptide, the cells were fixed, stained with crystal violet, and photographed (3 photographs per well) as described above. Both the total number of cells on each photograph and those with an elongated morphology (longest axis > 2 x shortest axis) were counted separately. The ratio of elongated to total cells was calculated. Each peptide was ranked according to its ability to reduce the percentage of elongated cells. All assays were done in duplicate.

*Measurement of tubulin polymerization*

A tubulin polymerization kit that measures the aggregation of purified bovine tubulin (Millipore Corp., Burlington, MA), was used to examine the effects of KTH-222 on tubulin dynamics. The method employed by this kit was adapted from the methods of Sharansky et al. and Lee et al. [22, 23]. The degree of polymerization is based on the proportionality between the light scattered by microtubules, measured as turbidity, and the concentration of microtubule polymer. The test agents or their vehicles were added to a solution containing tubulin monomers in an appropriate buffer. The positive control, paclitaxel, was used at a concentration of 10 μm, as recommended by supplier of the kit. This mixture was incubated at 37°C in a microtiter plate and its optical density was measured at 350 nm every 2 minutes for 40 minutes using a plate reader. The results from different experiments were normalized for average total polymerization under the control conditions. Time "0" was set as the last time point before an increase in polymerization in the control condition.

*Xenograft study*

The xenograft study was performed at Translational Drug Development (TD2, Scottsdale, AZ) using their standard protocol, which was approved by the TD2 institutional review board (Approved Study #TD3567). Female athymic nude mice were received at 4 weeks of age and were acclimated for at least 5 days prior to study initiation. The mice were housed in microisolator cages and maintained under specific, pathogen-free conditions. The mice were fed Toland Global Diet® 2920x irradiated laboratory animal diet, and autoclaved water was freely available. All procedures were carried out under the institutional guidelines of Translational Drug Development Institutional Animal Care and Use Committee, which conform to the Guide for the Care and Use of Laboratory Animals as adopted and promulgated by the U. S. National Institutes of Health (Protocol Number TD3567). Animals were identified using transponders.

The mice were inoculated subcutaneously in the right flank with 0.1 ml of a 50% media/50% Matrigel® mixture containing a suspension of $5 \times 10^6$ cells/mouse of MIA-PaCa-2 tumor cells. At time of inoculation, the mice were 5-6 weeks old. Tumor bearing animals were monitored and tumors were measured periodically until they reached the designated start size (> 125 mm³). Tumor width and length diameters were measured using a digital caliper. The measured values were digitally recorded using the animal study management software, Study Director. Tumor volumes were calculated utilizing the formula: Tumor volume (mm³) = (a × b²/2) where 'b' is the smallest diameter and 'a' is the largest diameter [24]. On the thirteenth day following inoculation, designated Study Day 1, forty mice with tumor sizes of 129-188 mm³ were randomized into four groups (n = 10), each with a mean of approximately 160 mm³, by random equilibration using Study Director (Day 1). Tumor volumes and body weights were recorded when the mice were randomized and were measured again twice weekly thereafter. Percent body weight change compared to study day one was calculated after subtracting tumor weight from overall weight. Clinical observations were made daily.

On Study Day 1, some mice begin receiving 1 ml/kg intravenous (tail vein) injections of KTH-
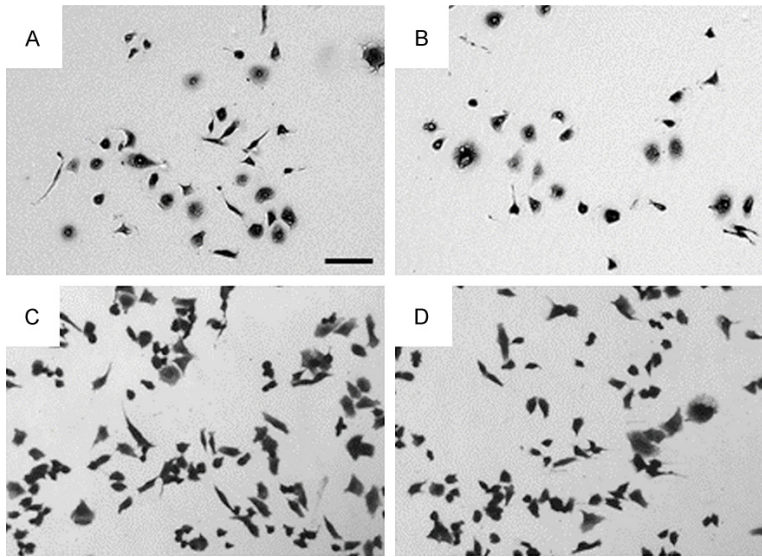
**Figure 1.** Effect of KTH-222 on cell morphology. Representative photomicrographs of HPAC (A and B) and MIA PaCA-2 (C and D) cells treated for 24 h with either KTH-222 (1 μM; B and D) or its vehicle (A and C) and then stained with crystal violet (see "Methods"). A decrease in the proportion of elongated cells can be appreciated following treatment with KTH-222. The bar at the lower right-hand corner of (A) indicates a length of 100 μm.

using t-tests. When multiple t-tests were done on the same data set, the probabilities were adjusted using the false discovery rate method of Benjamin and Hochberg [25].
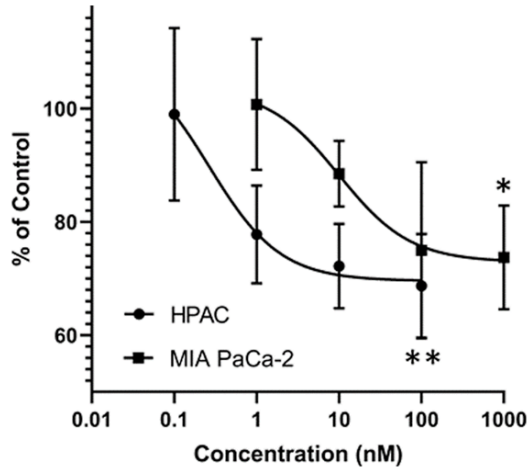
## Results

### Derivation of KTH-222

HPAC human pancreatic cancer cell cultures grown at low cell density were found to contain a majority of large, rounded cells and a smaller number of elongated, fusiform-shaped cells (**Figure 1A**). During pilot testing of ANP and related peptides for their actions on HPAC cells, the most obvious effect was a decrease in the percentage of elongated, fusiform cells in the culture (data not shown). The impact of KTH-222 treatment on HPAC cell morphology seen by comparing **Figure 1A** and **1B** illustrates this effect. Since a fibroblastic morphology has been associated with tumor invasiveness and metastasis [26], this reduction of cells with an elongated, fusiform shape was chosen as a measure of the potential anti-tumor activity of these peptides.

The sequences of ANP and the related peptides KP, LANP and VDL, which share a common precursor and which all inhibit the growth of cancer cells were compared, and an 8-amino acid length motif common to all of the peptides was identified (**Table 1**). A library of 96 8-mer peptides representing variations in the amino acids at each position that were consistent with the broad requirements of the motif was designed and synthesized. These peptides were then screened for their ability to reduce the percentage of elongated cells in HPAC cultures. The sequences of peptides that had greater activity (i.e. top tercile) were compared with the sequences of those that had lower active (i.e. bottom tercile). Individual amino acids or combinations of up to three amino acids that conferred greater or lower activity at each position within the motif were identified. A model of the optimally active peptide was constructed by incorporating those sequence elements that

222 (0.5 mg/ml), VDL (2 mg/ml), or their vehicle (Control group) three times weekly for the duration of the study. Other mice received the positive standard drug, gemcitabine, intraperitoneally at a dose of 80 mg/kg in a volume of 10 ml/kg. Gemcitabine was given once every 3 days for four cycles. This regimen for gemcitabine has been found to produce the maximum effectiveness possible in this model without causing lethality. Treatment groups were terminated when the average tumor volume for the group reached 1000 mm$^3$ (terminal tumor volume).

### Statistical comparisons

Grubb's test was used to identify animals in the xenograft study who were outliers from their group based on tumor growth. The outliers were eliminated from the study before further statistical analysis, resulting in the loss of one animal from each group except the VDL-treated group. The results from the xenograft study (after removal of the outliers) as well as the tubulin polymerization measurements were compared using a two-way ANOVA and post hoc comparisons with Bonferroni corrections for multiple comparisons (IBM SPSS® Statistics v. 25, IBM, Armonk, NY). Individual means from the *in vivo* and *in vitro* studies were compared

**Figure 2.** Reductions in the numbers of HPAC and MIA PaCA-2 cells after 24 h of exposure to KTH-222. Values are the mean and standard deviation of 5-7 different experiments (HPAC) or 4 different experiments (MIA PaCa-2). Curves were fit with GraphPad Prism 8® using a non-linear, three parameter model. The single and double asterisks indicate a significance difference from the control using a single sample t-test, with P < .001 (n = 7) and P < .05 (n = 4), respectively.

conferred greater activity and avoiding those associated with lower activity. Six peptides that fit this model were synthesized and tested in the same assay used for originally screening the peptide library. KTH-222 was found have the highest level of activity in this group. The other activities of KTH-222 against human cancer cells are described in further detail below.

*Effect of KTH-222 on cultured human pancreatic cancer cells*

In HPAC cultures, treatment with 1 uM KTH-222 for 24 h reduced the number of cells with an elongate morphology from 15.8 ± 3.0% (n = 5) to 6.0 ± 4.4% (n = 3) (compare **Figure 1A** and **1B**). This 60.3% reduction in elongated cells was statistically significant (2-tailed t-test, P < .05). MIA PaCa-2 human pancreatic cancer cell cultures, similarly to HPAC cells, also contained a majority of large, rounded cells and a smaller number of elongated, fusiform-shaped cells (**Figure 1C**). The effect of KTH-222 on MIA PaCa-2 cell cultures was qualitatively similar to that on HPAC cells (compare **Figure 1C** and **1D**).

Treatment of newly plated HPAC and MIA PaCa-2 with KTH-222 for 24 hours reduced the number of cells present in the culture com-

pared to control conditions (**Figure 2**). For both cell lines, this reduction was concentration dependent. For the HPAC cells, the inhibition appeared to plateau at 30 ± 10% at a KTH-222 concentration of 100 nM. This reduction was statistically significant (single-sample t-test compared to a value of 0, P < .001, n = 7). KTH-222 was less potent in reducing the number of MIA PaCa-2 cells in culture, with an apparent plateau in effect not being reached until a concentration of 1 mM. The reduction in cell number at this concentration was 26 ± 10%, which was also statistically significant (single-sample t-test compared to a value of 0, P < .05, n = 4). The 100 nM concentration of KTH-222 did not significantly reduce the percentage of viable HPAC cells compared to control treatment (78 ± 22% and 80 ± 16%, respectively, n = 5), nor did a 1 mM concentration of KTH-222 reduce the viability of MIA PaCa-2 cells (89 ± 4% viability of treated cells and 90 ± 5% of untreated, n = 4).

KTH-222 (1 µM) also reduced the ability of HPAC cells to attach to tissue culture-treated microtiter plates. Four hours after the plating of HPAC cells at a density of $5.0 \times 10^5$ cells/well in control medium, 54% of the cells (2.7 ± $1.8 \times 10^5$ cells) remained unattached as measured by counting cell in the medium. The presence of KTH-222 during these 4 hours increased the number of unattached HPAC to 72% (3.6 ± $1.8 \times 10^5$ cells). This increase of 18% was statistically significant (1-tailed t-test, P < .05, n = 3).

*Effect of KTH-222 on tubulin polymerization*

Under control conditions, tubulin polymerization accelerated rapidly after approximately 10 minutes of incubation and approached a plateau by 30 minutes (**Figure 3**). The positive standard for the tubulin polymerization assay, paclitaxel (10 uM), increased the total amount of polymerization compared to the vehicle, especially early in the polymerization period. The difference between the control and paclitaxel curves was statistically significant (P > .001; two-way ANOVA). This effect of paclitaxel on tubulin polymerization is consistent with reported results [27]. In contrast, KTH-222 produced a decrease in tubulin polymerization. This inhibition appeared to be concentration dependent and the reduction produced by 1
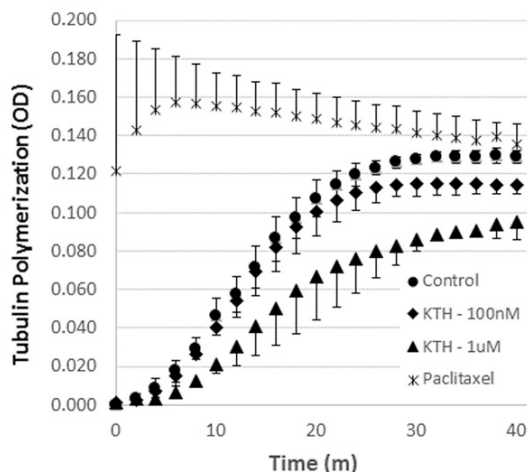
**Figure 3.** Effect of KTH-222 on tubulin association. Polymerization was conducted in the presence of paclitaxel (the positive standard; 10 µM; n = 5), KTH-222 (100 nM and 1 uM; n = 2, each) or the vehicle (Control; n = 6). The curves for both paclitaxel and 1 uM KTH-222 significantly differed from the control curve and from each other (P < .001; two-way ANOVA). The difference between the 100 nM KTH-222 curve and the control curve was not statistical significance.

uM KTH-222 was statistically significantly (two-way ANOVA, P < .001).

*Effect of KTH-222 on human pancreatic tumor growth in a xenograft model*

Gemcitabine treatment (80 mg/kg IP, given once every 3 days for four cycles) reduced the rate of tumor growth in mice implanted with MIA PaCa-2 human pancreatic cancer cells compared to control treatment (two-way ANOVA, P < .001; **Figure 4**). A maximum decrease in tumor volume of 29% was reached five days after the final dose of gemcitabine (Study Day 17). This decrease was statistically significant (2-tailed t-test, P < .01). After this point, the percentage reduction in tumor volume declined to a value of 14% by Study Day 45 (not statistically significant). No measures of effectiveness compared to controls could be made after Study Day 45 because the control group reached its terminal tumor volume on this day and was terminated. The gemcitabine-treated group reached its terminal tumor volume on Study Day 52, one week after the control group had reached this point.

KTH-222 treatment (0.5 mg/kg IV, three times weekly for the duration of the study) also resulted in a reduced rate of tumor growth com-
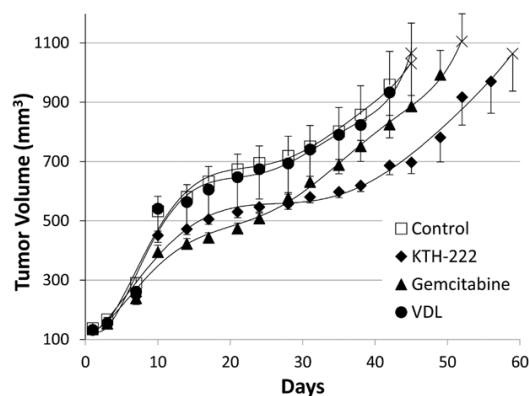


**Figure 4.** Reduction of human pancreatic cancer growth in a mouse xenograft model produced by KTH-222. The tumor growth curves for KTH-222 and gemcitabine treatments were both significantly different than that for control treatment (two-way ANOVA, P < .001). The curve for VDL treatment did not differ from that for control treatment (two-way ANOVA, P = 1.00). Starting at Study Day 30 and proceeding until the gemcitabine group reached their terminal tumor volume (Study Day 52), the curve for tumor growth in animals treated with KTH-222 was also significantly different than that for those animals treated with gemcitabine (see "Methods"). Group mean values and standard deviations are shown. "X" indicates the point at which the terminal tumor volume for each group was reached or first exceeded (see "Methods").

pared to control treatment (two-way ANOVA, P < .001; **Figure 4**). The percentage of reduction increased throughout the treatment period and reached a maximum of 31% on Study Day 45. This reduction was statistically significant (2-tailed t-test, P < .05). From Study Day 30 onward, KTH-222 treatment produced a significantly greater reduction in tumor growth than did gemcitabine treatment (two-way ANOVA, P < .001). KTH-222-treated animals did not reach terminal tumor volume until day 59, two weeks later than the control group and one week later than gemcitabine-treated group.

Vessel dilator (VDL) is one of the peptides related to ANP by having a common precursor and has been reported to be more effective than ANP in reducing the growth of human pancreatic cancer cells in a mouse xenograft model [18]. In the present study, VDL treatment only produced a small decrease in tumor volume. This decrease reached a maximum of 4.9% on Study Day 17 which was not statistically significant. The VDL-treated group reached termi-

nal tumor volume on the same Study Day as the control group (Study Day 45, **Figure 4**).

Animals treated with gemcitabine experienced their maximum weight loss on Study Day 7, which was during the gemcitabine treatment period that extended from Study Day 1 to 10. On Study Day 7, the average weight (after subtraction of tumor weight) of the gemcitabine-treated animals was 21.2 ± 2.3 g and that of the control animals was 22.9 ± 1.4. This compares to weights of 22.7 ± 2.2 g and 22.7 ± 1.4 g, respectively, on Study Day 1. The reduction in weight in the gemcitabine group, while moderate (7.4%), was a statistically significant decrease (one-tailed t-test, P < .05). Animals treated with KTH-222 experienced their maximum weight loss on Study Day 3. Their weight, however, did not differ from that of the control group (22.6 ± 1.5 and 22.6 ± 2.1, respectively) since the control group also lost weight on Study Day 3.

## Discussion

KTH-222 is a novel, small peptide whose sequence is based on an 8-amino acid long motif present in ANP and a group of related peptides, all of which reduce cancer cell growth [9-12, 14-17, 19, 28]. This motif is defined primarily by the chemical characteristics of the amino acid side chains at certain key locations (e.g. polar vs. non-polar) rather than by specific amino acids. Despite the imprecision in its definition, we feel that it is the most plausible mechanism for the common action of these peptides. We focused on the 8-amino acid length motif itself rather than also considering the flanking regions present in ANP and others of the related peptides because, even using just this truncated peptide, the range of substitution patterns to be explored was very large. The finding that KTH-222 was more active than in a xenograft model system than one of the full-length ANP-related peptides containing the natural version of the motif (VDL) at least partly validates this approach.

We initially observed that ANP-related peptides, including those of our motif-based peptide library, primarily affected HPAC and MIA PaCa-2 cell morphology. KTH-222 also produced decreases in cell attachment to the plate and, possibly as a consequence, cell number 24 hours later. Surprisingly, KTH-222 did not re-

duce cell viability. While the latter finding is consistent with reports showing minimal toxicity of ANP-related peptides on normal cells [29-31], it disagrees with other studies showing modest to profound toxic effects against cancer cells [11-13]. The *in vitro* studies in the present report employed a lower concentration of peptide and a shorter exposure time than the cytotoxicity assays used in some other studies. These differences could have reduced our ability to observe cytotoxic effects. Alternatively, the primary mechanism of reduced cancer cell growth by these peptides may not be cytotoxicity.

One potential common thread between the three *in vitro* actions of KTH-222 observed in the present study (i.e. altered morphology, reduced attachment, attenuated proliferation) is altered tubulin functioning [32, 33]. We, therefore examined the effect of KTH-222 on tubulin dynamics and found that it inhibited tubulin polymerization. Other drugs that disrupt tubulin dynamics, such as the taxanes and vinca alkaloids, are thought to interfere with the functioning of the centromere and, thereby, produce cytotoxicity [34-36]. Our finding that KTH-222 reduced cell number with no change in viability suggests a different mechanism for this peptide. It is likely that KTH-222 is internalized by cells through bindings to the NPR-C receptor in the same manner as ANP [37]. It is unlikely, however, that it is able to enter the nucleus and interfere with centromere function because of its relatively large size. Thus, KTH-222 may act primarily on cytoplasmic tubulin. Although the anti-tubulin effects of KTH-222 do provide a possible basis for its activities on cancer cells, many other biochemical activities have been reported for ANP and its related peptides which could also contribute to reduced cancer cell growth [9, 11, 38-40]. The effects of KTH-222 on some of these other mechanisms are under investigation.

In the xenograft system, gemcitabine produced a maximal decrease in tumor volume of 29% and extended survival time by one week compared to control treatment. This reduction of tumor volume was smaller than expected. In a pilot study using the same xenograft model system, gemcitabine produced a much larger maximal decrease in tumor volume compared to control treatment (61%) but the same one-week extension in survival time (data not sh-

own). The reason for the variability in the effectiveness of gemcitabine in reducing tumor volume between these two studies is not known. The extension of survival time produced by gemcitabine was, however, consistent.

The dosage of KTH-222 used in the xenograft study was selected to produce a 1 µM concentration in the body fluid, assuming a one-compartment model for distribution and a total fluid volume of approximately 55% of body weight [41]. This concentration was selected based on *in vitro* potency of the peptide. KTH-222 at this dose was more effective than gemcitabine in reducing the growth of human pancreatic cancer cell tumors. In particular, KTH-222 produced a significantly greater reduction of tumor growth than gemcitabine in the latter part of the study. Furthermore, KTH-222 extended a survival time longer than did gemcitabine.

One gross indicator of mouse health is weight maintenance or gain. The gemcitabine-treated group in our xenograft study experienced a modest, but statistically significant weight loss (7.4%) compared to the control group during the gemcitabine administration period. This small degree of this loss is consistent with the gemcitabine dose having been chosen to limit gross toxicity. Surprisingly, KTH-222 produced no weight loss relative to control treatment during its administration period. This suggests that it may be relatively free of gross toxic effects.

VDL, given at the same molar dosage as KTH-222, produced only a 4.9% decrease tumor growth in MIA PaCa-2 xenograft model. These findings seem to disagree with two earlier studies in which VDL was reported to produce greater than a 90% reduction in tumor growth in xenografts implanted with HPAC cells [17, 18]. In one of these studies [17], VDL was given as an IV bolus, as it was in the present study. One possible explanation for this discrepancy is that MIA PaCa-2 xenografts are more resistant than HPAC xenografts to the effects of VDL. Another possible explanation lies in differences in the method of implanting the tumor cells between the studies. The earlier studies used a smaller number of tumor cells ($10^6$) which were injected in phosphate-buffered saline [17]. Our study employed a more common protocol of injecting a larger number of cells ($5 \times 10^6$) in a 50% Matrigel® matrix. The latter approach facilitates production of a tumor by the cells [42]. In addition, treatment in our study began after the tumors had reached a larger size than in the earlier studies. The larger size and more established nature of the tumors in our xenograft system may also have reduced the effectiveness of VDL.

The ability of KTH-222 to inhibit tubulin polymerization may be particularly useful in the treatment of pancreatic cancer as well as other cancers in which tubulin inhibitors, such as nab paclitaxel have proven to be effective [5, 7, 43-49]. KTH-222 could also be useful in inhibiting cancer cell metastasis. Thus, it might interfere with the changes in cancer cell adhesion properties that are critical in the formation of metastases [50, 51]. In addition, by interfering with changes in cell morphology it may inhibit the adoption of a mesenchymal phenotype by cancer cells that makes them more invasive [26]. Inhibition of cancer cell metastasis has been reported when using ANP to treat postoperative lung cancer patients [20].

The utility of many currently used drugs in treating pancreatic cancer is ultimately limited by their toxicities and the eventual development of resistance to their actions [35, 52, 53]. KTH-222 has the potential to be less toxic, and may be less susceptible to the development of resistance based its peptidic chemical structure [54]. Thus KTH-222 or other peptides of its class may be useful additions to current chemotherapies.

## Disclosure of conflict of interest

None.

Address correspondence to: Michael R Kozlowski, Arizona College of Optometry, Midwestern University, Glendale, Arizona, United States of America. E-mail: mkozlo@midwestern.edu

## References

[1] Yabar CS and Winter JM. Pancreatic cancer: a review. Gastroenterol Clin North Am 2016; 45: 429-45.

[2] Varadhachary GR and Wolff RA. Current and evolving therapies for metastatic pancreatic cancer: are we stuck with cytotoxic chemotherapy? J Oncol Pract 2016; 12: 797-805.

[3] Wachtel MS, Xu KT, Zhang Y, Chiriva-Internati M and Frezza EE. Pancreas cancer survival in the gemcitabine era. Clin Med Oncol 2008; 2: 405-13.

[4] Adel N. Current treatment landscape and emerging therapies for pancreatic cancer. Am J Manag Care 2019; 25: S3-S10.

[5] Mukhtar E, Adhami VM and Mukhtar H. Targeting microtubules by natural agents for cancer therapy. Mol Cancer Ther 2014; 13: 275-84.

[6] Orr GA, Verdier-Pinard P, McDaid H and Horwitz SB. Mechanisms of Taxol resistance related to microtubules. Oncogene 2003; 22: 7280-95.

[7] Zhang Y, Yang SH and Guo XL. New insights into Vinca alkaloids resistance mechanism and circumvention in lung cancer. Biomed Pharmacother 2017; 96: 659-666.

[8] Sherrod AM, Brufsky A and Puhalla S. A case of late-onset gemcitabine lung toxicity. Clin Med Insights Oncol 2011; 5: 171-6.

[9] Lelievre V, Pineau N, Hu Z, Ioffe Y, Byun JY, Muller JM and Waschek JA. Proliferative actions of natriuretic peptides on neuroblastoma cells. Involvement of guanylyl cyclase and non-guanylyl cyclase pathways. J Biol Chem 2001; 276: 43668-76.

[10] Rashed HM, Sun H and Patel TB. Atrial natriuretic peptide inhibits growth of hepatoblastoma (HEP G2) cells by means of activation of clearance receptors. Hepatology 1993; 17: 677-84.

[11] Vesely DL. Cardiac hormones for the treatment of cancer. Endocr Relat Cancer 2013; 20: R113-25.

[12] Baldini PM, Lentini A, Mattioli P, Provenzano B, De Vito P, Vismara D and Beninati S. Decrease of polyamine levels and enhancement of transglutaminase activity in selective reduction of B16-F10 melanoma cell proliferation induced by atrial natriuretic peptide. Melanoma Res 2006; 16: 501-7.

[13] Zhang J, Zhao Z, Zu C, Hu H, Shen H, Zhang M and Wang J. Atrial natriuretic peptide modulates the proliferation of human gastric cancer cells via KCNQ1 expression. Oncol Lett 2013; 6: 407-414.

[14] Ohsaki Y, Yang HK, Le PT, Jensen RT and Johnson BE. Human small cell lung cancer cell lines express functional atrial natriuretic peptide receptors. Cancer Res 1993; 53: 3165-71.

[15] Serafino A, Moroni N, Psaila R, Zonfrillo M, Andreola F, Wannenes F, Mercuri L, Rasi G and Pierimarchi P. Anti-proliferative effect of atrial natriuretic peptide on colorectal cancer cells: evidence for an Akt-mediated cross-talk between NHE-1 activity and Wnt/beta-catenin signaling. Biochim Biophys Acta 2012; 1822: 1004-18.

[16] Bell EN, Tse MY, Frederiksen LJ, Gardhouse A, Pang SC, Graham CH and Siemens DR. Atrial natriuretic peptide attenuates hypoxia induced chemoresistance in prostate cancer cells. J Urol 2007; 177: 751-6.

[17] Lenz A, Sun Y, Eichelbaum EJ, Skelton WP 4th, Pi G and Vesely DL. Twice-weekly intravenous treatment of pancreatic cancer with atrial natriuretic peptide and vessel dilator. In Vivo 2010; 24: 125-9.

[18] Vesely DL, Eichelbaum EJ, Sun Y, Alli AA, Vesely BA, Luther SL and Gower WR Jr. Elimination of up to 80% of human pancreatic adenocarcinomas in athymic mice by cardiac hormones. In Vivo 2007; 21: 445-51.

[19] Eichelbaum EJ, Sun Y, Alli AA, Gower WR Jr and Vesely DL. Cardiac and kidney hormones cure up to 86% of human small-cell lung cancers in mice. Eur J Clin Invest 2008; 38: 562-70.

[20] Nojiri T, Hosoda H, Tokudome T, Miura K, Ishikane S, Otani K, Kishimoto I, Shintani Y, Inoue M, Kimura T, Sawabata N, Minami M, Nakagiri T, Funaki S, Takeuchi Y, Maeda H, Kidoya H, Kiyonari H, Shioi G, Arai Y, Hasegawa T, Takakura N, Hori M, Ohno Y, Miyazato M, Mochizuki N, Okumura M and Kangawa K. Atrial natriuretic peptide prevents cancer metastasis through vascular endothelial cells. Proc Natl Acad Sci U S A 2015; 112: 4086-91.

[21] Kozlowski MR. Anti-cell proliferative compounds and methods of use, U.S. Patent #9,808,512, 2017.

[22] Shelanski ML, Gaskin F and Cantor CR. Microtubule assembly in the absence of added nucleotides. Proc Natl Acad Sci U S A 1973; 70: 765-8.

[23] Lee JC and Timasheff SN. In vitro reconstitution of calf brain microtubules: effects of solution variables. Biochemistry 1977; 16: 1754-64.

[24] Euhus DM, Hudd C, LaRegina MC and Johnson FE. Tumor measurement in the nude mouse. J Surg Oncol 1986; 31: 229-34.

[25] Benjamini Y and Hochberg Y. Controlling the false discovery rate - a practical and powerful approach to multiple testing. J R Stat Soc Series B Stat Methodol 1995; 57: 289-300.

[26] Friedl P and Wolf K. Tumour-cell invasion and migration: diversity and escape mechanisms. Nat Rev Cancer 2003; 3: 362-74.

[27] Schiff PB, Fant J and Horwitz SB. Promotion of microtubule assembly in vitro by taxol. Nature 1979; 277: 665-7.

[28] Lenz A, Sun Y, Eichelbaum EJ, Skelton WP 4th, Pi G and Vesely DL. Cardiac hormones elimi-

nate some human squamous lung carcinomas in athymic mice. Eur J Clin Invest 2010; 40: 242-9.

[29] Hamad AM, Johnson SR and Knox AJ. Antiproliferative effects of NO and ANP in cultured human airway smooth muscle. Am J Physiol 1999; 277: L910-8.

[30] Skelton WP 4th, Pi GE and Vesely DL. Four cardiac hormones cause death of human cancer cells but not of healthy cells. Anticancer Res 2011; 31: 395-402.

[31] Kiemer AK and Vollmar AM. Effects of different natriuretic peptides on nitric oxide synthesis in macrophages. Endocrinology 1997; 138: 4282-90.

[32] Omelchenko T, Vasiliev JM, Gelfand IM, Feder HH and Bonder EM. Mechanisms of polarization of the shape of fibroblasts and epitheliocytes: Separation of the roles of microtubules and Rho-dependent actin-myosin contractility. Proc Natl Acad Sci U S A 2002; 99: 10452-7.

[33] Rodionov VI, Gyoeva FK, Tanaka E, Bershadsky AD, Vasiliev JM and Gelfand VI. Microtubule-dependent control of cell shape and pseudopodial activity is inhibited by the antibody to kinesin motor domain. J Cell Biol 1993; 123: 1811-20.

[34] Gligorov J and Lotz JP. Preclinical pharmacology of the taxanes: implications of the differences. Oncologist 2004; 9 Suppl 2: 3-8.

[35] Gascoigne KE and Taylor SS. How do anti-mitotic drugs kill cancer cells? J Cell Sci 2009; 122: 2579-85.

[36] Kelling J, Sullivan K, Wilson L and Jordan MA. Suppression of centromere dynamics by Taxol in living osteosarcoma cells. Cancer Res 2003; 63: 2794-2801.

[37] Potter LR. Natriuretic peptide metabolism, clearance and degradation. FEBS J 2011; 278: 1808-17.

[38] Segawa K, Minami K, Jimi N, Nakashima Y and Shigematsu A. C-type natriuretic peptide inhibits rat mesangial cell proliferation by a phosphorylation-dependent mechanism. Naunyn Schmiedebergs Arch Pharmacol 1998; 357: 70-6.

[39] Pandey KN, Nguyen HT, Li M and Boyle JW. Natriuretic peptide receptor-A negatively regulates mitogen-activated protein kinase and proliferation of mesangial cells: role of cGMP-dependent protein kinase. Biochem Biophys Res Commun 2000; 271: 374-9.

[40] Panayiotou CM and Hobbs AJ. C-Type natriuretic peptide mediates ERK1/2 phosphorylation via Gi-coupled natriuretic peptide receptor-C in rat aortic smooth muscle cells. Acta Pharmacologica Sinica 2006; 27: 170-170.

[41] Chapman ME, Hu L, Plato CF and Kohan DE. Bioimpedance spectroscopy for the estimation of body fluid volumes in mice. Am J Physiol Renal Physiol 2010; 299: F280-3.

[42] Mullen P. The use of matrigel to facilitate the establishment of human cancer cell lines as xenografts. Methods Mol Med 2004; 88: 287-92.

[43] Fauzee NJ. Taxanes: promising anti-cancer drugs. Asian Pac J Cancer Prev 2011; 12: 837-51.

[44] Moudi M, Go R, Yien CY and Nazre M. Vinca alkaloids. Int J Prev Med 2013; 4: 1231-5.

[45] Stanton RA, Gernert KM, Nettles JH and Aneja R. Drugs that target dynamic microtubules: a new molecular perspective. Med Res Rev 2011; 31: 443-81.

[46] Liebmann JE, Cook JA, Lipschultz C, Teague D, Fisher J and Mitchell JB. Cytotoxic studies of paclitaxel (Taxol) in human tumour cell lines. Br J Cancer 1993; 68: 1104-9.

[47] Pauwels O, Kiss R, Pasteels JL and Atassi G. Cytotoxicity, cell cycle kinetics and morphonuclear-induced effects of Vinca alkaloid anticancer agents. J Pharm Pharmacol 1995; 47: 870-5.

[48] Villena-Heinsen C, Friedrich M, Ertan AK, Farnhammer C and Schmidt W. Human ovarian cancer xenografts in nude mice: chemotherapy trials with paclitaxel, cisplatin, vinorelbine and titanocene dichloride. Anticancer Drugs 1998; 9: 557-63.

[49] Yamori T, Sato S, Chikazawa H and Kadota T. Anti-tumor efficacy of paclitaxel against human lung cancer xenografts. Jpn J Cancer Res 1997; 88: 1205-10.

[50] Korb T, Schluter K, Enns A, Spiegel HU, Senninger N, Nicolson GL and Haier J. Integrity of actin fibers and microtubules influences metastatic tumor cell adhesion. Exp Cell Res 2004; 299: 236-47.

[51] Brooks SA, Lomax-Browne HJ, Carter TM, Kinch CE and Hall DM. Molecular interactions in cancer cell metastasis. Acta Histochem 2010; 112: 3-25.

[52] Lee H, Park S, Kang JE, Lee HM, Kim SA and Rhie SJ. Efficacy and safety of nanoparticle-albumin-bound paclitaxel compared with solvent-based taxanes for metastatic breast cancer: a meta-analysis. Sci Rep 2020; 10: 530.

[53] Tamura T, Sasaki Y, Nishiwaki Y and Saijo N. Phase I study of paclitaxel by three-hour infusion: hypotension just after infusion is one of the major dose-limiting toxicities. Jpn J Cancer Res 1995; 86: 1203-9.

[54] Nuti R, Goud NS, Saraswati AP, Alvala R and Alvala M. Antimicrobial peptides: a promising therapeutic strategy in tackling antimicrobial resistance. Curr Med Chem 2017; 24: 4303-4314.